JOURNAL OF BACTERIOLOGY, Feb. 1998, p. 969–978 Vol. 180, No. 4
0021-9193/98/$04.00+0


# Isolation and Characterization of *Rhodobacter capsulatus* Mutants Affected in Cytochrome $cbb_3$ Oxidase Activity

HANS-GEORG KOCH, OLIVIA HWANG, AND FEVZI DALDAL*

*Department of Biology, Plant Science Institute, University of Pennsylvania, Philadelphia, Pennsylvania 19104-6018*

Received 19 August 1997/Accepted 11 December 1997

**The facultative phototrophic bacterium *Rhodobacter capsulatus* contains only one form of cytochrome (cyt) *c* oxidase, which has recently been identified as a $cbb_3$-type cyt *c* oxidase. This is unlike other related species, such as *Rhodobacter sphaeroides* and *Paracoccus denitrificans*, which contain an additional mitochondrial-like $aa_3$-type cyt *c* oxidase. An extensive search for mutants affected in cyt *c* oxidase activity in *R. capsulatus* led to the isolation of at least five classes of mutants. Plasmids complementing them to a wild-type phenotype were obtained for all but one of these classes from a chromosomal DNA library. The first class of mutants contained mutations within the structural genes (*ccoNOQP*) of the cyt $cbb_3$ oxidase. Sequence analysis of these mutants and of the plasmids complementing them revealed that *ccoNOQP* in *R. capsulatus* is not flanked by the oxygen response regulator *fnr*, which is located upstream of these genes in other species. Genetic and biochemical characterizations of mutants belonging to this group indicated that the subunits CcoN, CcoO, and CcoP are required for the presence of an active cyt $cbb_3$ oxidase, and unlike in *Bradyrhizobium japonicum*, no active CcoN-CcoO subcomplex was found in *R. capsulatus*. In addition, mutagenesis experiments indicated that the highly conserved open reading frame 277 located adjacent to *ccoNOQP* is required neither for cyt $cbb_3$ oxidase activity or assembly nor for respiratory or photosynthetic energy transduction in *R. capsulatus*. The remaining cyt *c* oxidase-minus mutants mapped outside of *ccoNOQP* and formed four additional groups. In one of these groups, a fully assembled but inactive cyt $cbb_3$ oxidase was found, while another group had only extremely small amounts of it. The next group was characterized by a pleiotropic effect on all membrane-bound *c*-type cytochromes, and the remaining mutants not complemented by the plasmids complementing the first four groups formed at least one additional group affecting the biogenesis of the cyt $cbb_3$ oxidase of *R. capsulatus*.**

The gram-negative facultative photosynthetic bacterium *Rhodobacter capsulatus* has a highly branched electron transport chain, resulting in its ability to grow under a wide variety of conditions (52). Its light-driven photosynthetic electron transfer pathway is a cyclic process between the photochemical reaction center and the ubihydroquinone cytochrome (cyt) *c* oxidoreductase (cyt $bc_1$ complex) (30). On the other hand, the respiratory electron transfer pathways of *R. capsulatus* are branched after the quinone pool and contain two different terminal oxidases, previously called cyt $b_{410}$ (cyt *c* oxidase) and cyt $b_{260}$ (quinol oxidase) (3, 27, 29, 53). The branch involving cyt *c* oxidase is similar to the mitochondrial electron transfer chain in that it depends on the cyt $bc_1$ complex and a *c*-type cyt acting as an electron carrier. The quinol oxidase branch circumvents the cyt $bc_1$ complex and the cyt *c* oxidase by taking electrons directly from the quinone pool to reduce $O_2$ to $H_2O$. The pronounced metabolic versatility, including the ability to grow under dark, anaerobic conditions (50, 52), makes these purple non-sulfur bacteria excellent model organisms for studying microbial energy transduction.

Marrs and Gest (29) have reported the first *R. capsulatus* mutants which were defective in the respiratory electron transport chain. Of these mutants, M5 was incapable of catalyzing the α-naphthol plus *N*′,*N*′-dimethyl-*p*-phenylenediamine (DMPD) plus $O_2$→indophenol blue plus $H_2O$ reaction (NADI reaction) and unable to grow by respiration ($Res^-$), and hence was deficient in both terminal oxidases. Another mutant, M4, was also $NADI^-$ but $Res^+$ due to the presence of an active quinol oxidase. Marrs and Gest have also described two different spontaneous revertants of M5, called M6 and M7, which regained the ability to grow by respiration (29). M6 regained cyt *c* oxidase activity and became concurrently $NADI^+$ and sensitive to low concentrations of cyanide and the cyt $bc_1$ inhibitor myxothiazol, but remained quinol $oxidase^-$. On the other hand, M7 regained the quinol oxidase activity but remained cyt *c* $oxidase^-$ (thus, $NADI^-$ and resistant to myxothiazol, a phenotype identical to that of M4). All of these mutants remained proficient for phototrophic (Ps) growth.

The cyt *c* oxidase of *R. capsulatus* has been purified previously and characterized as being a novel $cbb_3$-type cyt *c* oxidase without a $Cu_A$ center (15). It is composed of at least a membrane-integral *b*-type cyt (subunit I [CcoN]) with a low-spin heme *b* and a high-spin heme $b_3$-$Cu_B$ binuclear center, and two membrane-anchored *c*-type cyts (CcoO and CcoP). It has a unique active site that possibly confers a very high affinity for its substrate oxygen (49). The structural genes of this enzyme (*ccoNOQP*) have been sequenced recently from *R. capsulatus* 37b4 (45) and aligned to the partial amino acid sequence of the purified enzyme from *R. capsulatus* MT1131 (15). Although a *ccoN* mutant of strain 37b4 was reported to lack cyt *c* oxidase activity (45), the observed discrepancies between the amino acid sequence and the nucleotide sequence do not entirely exclude the possible presence of two similar *cb*-type cyt *c* oxidases in this species. The presence of a similar cyt *c* oxidase has also been demonstrated in several other bacteria, including *P. denitrificans* (9), *R. sphaeroides* (13), and *Rhizobium* spp. In the latter species, the homologs of *ccoNOQP* have been named *fixNOQP* (23, 34) and are required to support respiration under oxygen-limited growth during symbiotic nitrogen fixation (36).

The biogenesis of a multisubunit protein complex containing

* Corresponding author. Mailing address: Department of Biology, Plant Science Institute, University of Pennsylvania, Philadelphia, PA 19104-6018. Phone: (215) 898-4394. Fax: (215) 898-8780. E-mail: fdaldal@mail.sas.upenn.edu.

several prosthetic groups, such as cyt $cbb_3$ oxidase, is likely to require many accessory proteins involved in various posttranslational events, including protein translocation, assembly, cofactor insertion, and maturation (46). Thus, insights into this important biological process, about which currently little is known, may be gained by searching for mutants defective in cyt *c* oxidase activity. In this work, we describe the isolation of such mutants and their molecular genetic characterization, including those already available, such as M4, M5, and M7G. These studies indicate that in *R. capsulatus*, gene products of at least five different loci are involved in the formation of an active cyt $cbb_3$ oxidase.

## MATERIALS AND METHODS

**Bacterial strains and growth conditions.** The strains and plasmids used in this study are described in Table 1. *Escherichia coli* strains and their plasmid-containing derivatives were grown in Luria-Bertani medium supplemented with antibiotics when appropriate (ampicillin, 100 μg/ml; kanamycin, 50 μg/ml; tetracycline, 12.5 μg/ml) (38). *R. capsulatus* strains were grown in Sistrom's minimal medium A (Med A) (42) or MPYE enriched growth medium (7) (both supplemented with kanamycin [10 μg/ml] or tetracycline [0.625 μg/ml] as needed) (21) at 35°C chemoheterotrophically under aerobic conditions in the dark on plates or liquid cultures (shaken at 150 rpm), or photoheterotrophically in the presence of light under anaerobiosis with $H_2$- and $CO_2$-generating gas packs from BBL Microbiology Systems, Cockeysville, Md.

**Bacterial and molecular genetic techniques.** *R. capsulatus* strains were mutagenized at 37°C for approximately 30 min with 100 mM ethyl methanesulfonate (EMS) dissolved in 100 mM $KH_2PO_4$ buffer (pH 7.4) as described earlier (7). In a typical screen, about 20 independent cultures on MPYE medium were inoculated with mutagenized cells, grown overnight under respiratory growth (Res) conditions, spread on MPYE plates to yield several hundred colonies per plate, and incubated under Ps conditions for 48 h. Well-pigmented visible colonies were marked, and plates were further incubated under Res conditions for an additional 24 to 48 h. Newly arising small and less-pigmented colonies were picked and tested for their Ps and Res phenotypes. All mutagenized colonies were also tested for their cyt *c* oxidase activity by the NADI reaction by being overlaid with a 1:1 (vol/vol) mixture of 35 mM α-naphthol in ethanol and 30 mM *N*,*N*-dimethyl-*p*-phenylene diamine in $H_2O$ (25). Under these conditions, colonies that contain an active cyt *c* oxidase (i.e., $NADI^+$) turn blue within 30 s. All $NADI^-$ or $Ps^-$ mutants were retained, but only the $Ps^+$ and $NADI^-$ mutants were further analyzed.

Conjugal transfer of plasmids from *E. coli* to *R. capsulatus*, interposon mutagenesis (with $Kan^r$ genes of pMA117 and pUC4-Kixx) via the gene transfer agent (GTA) (51), and Tn*5* mutagenesis were performed as described previously (7, 41). Standard molecular biology techniques were performed as described by Sambrook et al. (38). The plasmid p5TΔH was obtained by deletion of appropriate fragments of p5T, and p4AIV was obtained by ligation of the 3.4-kb *Bgl*II-*Bam*HI fragment of p4A into *Bam*HI-digested pRK404 (Fig. 1). pMG1 was constructed by insertion of the 1.3-kb *Bam*HI fragment of p5TΔH into the appropriate site of pBluescript ($KS^+$), and its cloning in two different orientations into pRK404 yielded pRHK8 and pRHK9. Insertion of the $Kan^r$ cartridge of pMA117 into the unique *Bst*EII site of pMG1 led to pMG1K, and the *ccoP::kan* allele thus obtained was introduced into the chromosome of the wild-type strain, MT1131, via GTA crosses and yielded the mutant MG1 (*ccoP*::*kan*). Cloning of the $Kan^r$-mediating chromosomal DNA fragment of MG1 into pBSII led to the isolation of pMG1-H1, and the location of the $Kan^r$ cartridge was determined by DNA sequencing. p4AXI was constructed by ligation of the 1.1-kb *Bgl*II-*Hin*dIII fragment of p4AIV into pRK415, and to obtain pOX15, the 1.3-kb *Bam*HI fragment of pMG1 was ligated to *Bam*HI-digested p4AIV (Fig. 1). The insertion-deletion mutant GK32 [Δ(*cco*NO::*kan*)] was constructed by replacement of the 2.8-kb *Xho*I fragment of p4AIV (carrying open reading frame 277 [ORF277] and *ccoNO*) with the $Kan^r$ gene and was introduced into the chromosome of MT1131 via GTA crosses. PCR was performed with *Taq* DNA polymerase after optimization with the Opti-Prime kit from Stratagene in a mixture containing 10 mM Tris-HCl (pH 8.8), 1.5 mM $MgCl_2$, 75 mM KCl, 15% glycerol, and 0.25 mM deoxynucleoside triphosphates. Fifteen picomoles of primer and 300 ng of genomic DNA were cycled 30 times (98°C for 30 s, 60°C for 10 s, and 72°C for 60 to 120 s) with a Perkin-Elmer 9600 GeneAmp PCR system.

**DNA sequence analysis.** Automated DNA sequencing with the dye terminator cycle sequencing kit (Amplitaq FS) from Applied Biosystems was performed as specified by the manufacturer. Various subclones of the plasmids described in Table 1 were used as double-stranded DNA templates with the following primers (shown in the 5′-to-3′ orientation) synthesized either at the DNA Synthesis Service, Department of Chemistry, University of Pennsylvania, or ordered from Gibco-BRL: MG1A, CCCGTGGCAAGTCGCTG; MG1B, CCCGCCGATCA TGGCCA; MG1C, GCGCAGTGCCACGGCGC; MG1D, CGAGCTGCTTGA ACCGGCGCA; MG1MA, AGCTCCAGGACGGCATCAC; MG1MB, ACCT GCTGACCCGCGGTCGC; MG1MO, TCATTGTCGGTTTGCCTAGG; N1, CTCCGGCCGAATCGTCGGGACGGGATT; N2, CGAAGACGGCCAATC TCGCCGTTGCGG; N3, CGGCAACGGGATGCTGAACT; N4, CCAAATC GGTGCAGCTGATG; N5, GCTCAACTGGCGGAACTAGC; N6, CGAGGA AGGCGATCAGATAG; N7, ACAAGAAAGCCGACGATCC; p4A3, TCGCG GATGTAGATGTCCCG; p4A4, CTTCGACGGTGGCGGCCAG; O1, ACCA GCTAAAGAGCTGGAAGGTTGGGC; O2, GCGATCGCGGTCACATCCG TCGCCACC; O3, TTCGACAGGTGTTCGACATGCC; O4, TGGCATGTCG AACACCTGTC; BHK20MD, AGCCGGCACCGGCACCGAGC; BHK20MC, GCTAGGCGTTCCGCGACGGC; BHK33MA, TTCGCACCACATCGG; BK33A, CCCGTCTCCTTGAAGGA; BK33B, CCCGCCACAAGGCACA; BK33C, ACAAGGAGCCAGCCCATG; BK33D, CCGGCGGCGCAGGCG GC; and BHK20B, CCAGTCGGGCAGCGCGGTAT.

DNA analyses, predictions for segmental flexibility in amino acid sequences, and homology searches were done with the MacVector (IBI, Kodak) and BLAST programs (2). The computer programs TmPred (18) and Clustal W (44) were used to predict the possible transmembrane helices and for sequence alignments, respectively.

**Construction of a *ccoN::lacZ* fusion.** A *ccoN::lacZ* translational fusion was constructed by PCR cloning of the 0.28-kb ORF277-*ccoN* intergenic region into the conjugative promoter-probe vector pXCA601 containing an in-frame *Bam*HI site at the 5′ end of *lacZ* (1). Briefly, this region was amplified by *Taq* DNA polymerase with 200 ng of the primers CNL (5′CAT TCT GCA GTT AGG TTA ACG GGT GCC GTC3′) and CNR-1 (5′GGC AAT AGG ATC CAC GAC GCC AAG AGC GAC AAG3′) in the presence of 20 ng of pOX15 as DNA template as described above, except that 50 mM (each) deoxynucleoside triphosphate was used. The reaction mixture was incubated at 98°C for 30 s prior to cycling (30 cycles of 97°C for 30 s, 55°C for 10 s, and 72°C for 60 s); the PCR product thus obtained was digested with *Pst*I and *Bam*HI restriction enzymes and cloned into the corresponding sites of pXCA601. The resulting plasmid, pXG2, carried the 280-bp DNA fragment containing the ORF277-*ccoN* intergenic region to yield an in-frame *ccoN::lacZ* translational fusion (see Fig. 3).

**Isolation of chromatophore membranes, SDS-PAGE and Western blot analysis, enzyme purification, and antibody production.** Chromatophore membranes were prepared in 20 mM MOPS [3-(*N*-morpholino)propanesulfonic acid] buffer (pH 7) containing 100 mM KCl with a French pressure cell as described earlier (15). The cyt $cbb_3$ oxidase was purified to homogeneity from semiaerobically grown *R. capsulatus* cells as described by Gray et al. (15). Sodium dodecyl sulfate-polyacrylamide gel electrophoresis (SDS-PAGE) was performed as described elsewhere (39) with 16.5 or 10% polyacrylamide gels. Samples were solubilized in 2% SDS and 5% β-mercaptoethanol and incubated for either 15 min at 75°C for Coomassie staining and Western blots, or 5 min at 37°C for visualization of *c*-type cyts with 3,3′,5,5′-tetramethylbenzidine (TMBZ) (43). For Western blot analysis, proteins were electroblotted onto Immobilon-P membranes (Millipore Corp., Bedford, Mass.) and immunoglobulins bound to cross-reacting *R. capsulatus* proteins were detected with horseradish peroxidase-conjugated goat anti-rabbit secondary antibodies (Bio-Rad, Richmond, Calif.). Diaminobenzidine was used as a peroxidase substrate enhanced with $NiCl_2$.

A preparative SDS-PAGE system (model 491 Prep Cell; Bio-Rad) was used to isolate the individual subunits of this enzyme as follows. Ten milligrams of purified cyt $cbb_3$ oxidase was applied to a 12% gel, which was then electrophoresed over 40 h at 8 W of constant power. The individual subunits were eluted in 25 mM Tris–200 mM glycine buffer (pH 8.3) with 0.1% SDS at a flow rate of 20 ml/h. For a rapid screening, 0.3 ml of the individual fractions was precipitated with 1.0 ml of acetone at −20°C for at least 8 h, washed once with acetone, resuspended in Tris-buffered saline (TBS) (50 mM Tris-HCl, 150 mM NaCl [pH 7.4]) buffer, and analyzed by SDS-PAGE with subsequent Coomassie and TMBZ stains. The fractions identified as containing the individual cyt *c* oxidase subunits were dialyzed three times against TBS buffer, lyophilized, resuspended in TBS buffer at a concentration of 1 mg/ml, and used to immunize New Zealand White rabbits. For primary injections, 100 μg of protein mixed with complete Freund's adjuvant was used, and for the subsequent booster injections, 50 μg of protein in incomplete Freund's adjuvant was used, and antibody titers were monitored periodically.

**Enzyme assays.** *N*,*N*,*N*′,*N*′ Tetramethyl-*p*-phenylenediamine (TMPD) oxidase activity was measured polarographically with a Clark-type oxygen electrode (YSI, Inc., Yellow Springs, Ohio) with *R. capsulatus* chromatophore membranes at a protein concentration of approximately 0.1 mg/ml in 50 mM MOPS buffer (pH 7) and 5 mM $MgCl_2$. Oxygen consumption induced by the addition of 10 mM ascorbate and 0.2 mM TMPD, and subsequently inhibited by 100 μM KCN, was recorded, and net TMPD oxidase activity was determined by subtraction of the endogenous respiratory rate from that induced by ascorbate. β-Galactosidase activity was measured with 100-μl samples of three independent cultures as described by Miller (31). Protein concentrations were determined by the method of Lowry (28).

**Chemicals.** All chemicals were of reagent grade and were obtained from commercial sources. Dodecyl β-D-maltoside was from Anatrace (Maumee, Ohio).

**Nucleotide sequence accession number.** The GenBank accession number for *ccoNOQP* of *R. capsulatus* and its surrounding genes is AF016223.

TABLE 1. Bacterial strains and plasmids used in this study

| Strain or plasmid | Genotype | Phenotype | Source or reference |
|---|---|---|---|
| Strains | | | |
| *E. coli* | | | |
| HB101 | F$^-$ *proA2 hsdS20* ($r_B^-$ $m_B^-$) *recA13 ara14 lacY1 galK2 rpsL20 supE44 rpsL20 supE44 proA2 xyl-5 mtl-1* | | 38 |
| XL1-Blue | *recA1 endA1 gyrA96 thi-1 hsdr17 supE44 relA1 lac*[F′ *proAB lacI*$^q$ΔM15 Tn*10*(Tet$^r$)] | | Stratagene |
| *R. capsulatus* | | | |
| MT1131[a] | *crtD121* Rif$^r$ | Wild type (NADI$^+$) | 40 |
| Y262 | | GTA overproducer | 51 |
| GK277-1 | ORF277-1::*kan* | Cox$^+$ NADI$^+$ | This work |
| GK277-2 | ORF277-2::*kan* | Cox$^+$ NADI$^+$ | This work |
| M4 | Δ*ccoN* | Cox$^-$ NADI$^-$ | 29 |
| M5 | *ccoNOQP qox* | Cox$^-$ Qox$^-$ NADI$^-$ | 29 |
| M7G | *ccoP269* | Cox$^-$ NADI$^-$ | 29 |
| MR1 | *ccoO107* | Cox$^-$ NADI$^-$ | This work |
| MG1 | *ccoP::kan* | Cox$^-$ NADI$^-$ | This work |
| OH2 | *ccoP* 34 | Cox$^-$ NADI$^-$ | This work |
| DB8 | *ccoP*::Tn*5* | Cox$^-$ NADI$^-$ | This work |
| GK32 | Δ(*ccoNO::kan*) | Cox$^-$ NADI$^-$ | This work |
| BK4 | *ccoNOQP*[b] | Cox$^-$ NADI$^-$ | This work |
| GK2 | *ccoNOQP*[b] | Cox$^-$ NADI$^-$ | This work |
| OH1 | *ccoNOQP*[b] | Cox$^-$ NADI$^-$ | This work |
| SS24 | *ccoNOQP*[b] | Cox$^-$ NADI$^-$ | This work |
| SS25 | *ccoNOQP*[b] | Cox$^-$ NADI$^-$ | This work |
| IW2 | *ccoNOQP*[b] | Cox$^-$ NADI$^-$ | This work |
| Sev1 | *ccoNOQP*[b] | Cox$^-$ NADI$^-$ | This work |
| Sev2 | *ccoNOQP*[b] | Cox$^-$ NADI$^-$ | This work |
| Sev3 | *ccoNOQP*[b] | Cox$^-$ NADI$^-$ | This work |
| Sev4 | *ccoNOQP*[b] | Cox$^-$ NADI$^-$ | This work |
| Sev5 | *ccoNOQP*[b] | Cox$^-$ NADI$^-$ | This work |
| BK5 | | Cox$^-$ NADI$^-$ | This work |
| SS33 | | Cox$^-$ NADI$^-$ | This work |
| SS1 | | Cox$^-$ NADI slow | This work |
| SS2 | | Cox$^-$ NADI slow | This work |
| MR2 | | Cox$^-$ NADI slow | This work |
| IJ1 | | Cox$^-$ NADI slow | This work |
| GK1 | | Cox$^-$ NADI$^-$ | This work |
| DM2 | | Cox$^-$ NADI slow | This work |
| IW3 | | Cox$^-$ NADI slow | This work |
| TP1 | | Cox$^-$ NADI slow | This work |
| TP2 | | Cox$^-$ NADI slow | This work |
| Plasmids | | | |
| pRK2013 | | Kan$^r$, helper | 10 |
| pRK415 | | Tet$^r$ | 10 |
| pRK404 | | Tet$^r$ | 10 |
| pBSII | pBluescript II (KS$^+$) | Amp$^r$ | Stratagene |
| pXCA601 | *lacZ* | Tet$^r$ | 1 |
| pMA117 | | Kan$^r$ | 7 |
| pUC4-Kixx | | Kan$^r$ | Pharmacia |
| p5T | pRK404 with a 16.5-kb *Bam*HI insert | Tet$^r$ | This work |
| p5TΔH | *Hin*dIII deletion of p5T | Tet$^r$ | This work |
| p4A | pRK404 with 6.0-kb *Bam*HI insert | Tet$^r$ | This work |
| p4AI | *Xho*I deletion of p4A | Tet$^r$ | This work |
| p4AIK32 | Kan$^r$ in *Xho*I site of p4AI | Kan$^r$ Tet$^r$ | This work |
| p4AIII | *Bgl*II deletion of p4A | Tet$^r$ | This work |
| p4AIIIK | Kan$^r$ in *Bgl*II site of p4AIII | Kan$^r$ Tet$^r$ | This work |
| p4AIV | 3.4-kb *Bgl*II-*Bam*HI fragment of p4A in pRK404 | Tet$^r$ | This work |
| p4AXI | 1.1-kb *Bgl*II-*Hin*dIII fragment of p4A in pRK404 | Tet$^r$ | This work |
| p4AXIK | Kan$^r$ in *Xho*I site of p4AXI | Kan$^r$ Tet$^r$ | This work |
| p4AXIIK | Kan$^r$ in *Nru*I site of p4AXI | Kan$^r$ Tet$^r$ | This work |
| pMG1 | 1.3-kb *Bam*HI fragment of p5TΔH in pBSII | Amp$^r$ | This work |
| pMG1K | Kan$^r$ in *Bst*EII site of pMG1 | Kan$^r$ Tet$^r$ | This work |
| pMG1-H1 | 10-kb *Hin*dIII fragment of MG1 in pBSII | Kan$^r$ Amp$^r$ | This work |
| pRHK8 | 1.3-kb *Bam*HI fragment of p5TΔH in pRK404, opposite orientation from that in p5TΔH | Tet$^r$ | This work |

*Continued on following page*

TABLE 1—*Continued*

| Strain or plasmid | Genotype | Phenotype | Source or reference |
|---|---|---|---|
| pRHK9 | 1.3-kb *Bam*HI fragment of p5TΔH in pRK404, same orientation as that in p5TΔH | Tet$^r$ | This work |
| pOX15 | 1.3-kb *Bam*HI fragment of p5TΔH cloned into *Bam*HI-digested p4AIV | Tet$^r$ | This work |
| pXG2 | ORF277-*ccoN::lacZ* | Tet$^r$ | This work |
| pBK1 | 4.5-kb *Hin*dIII fragment in pRK404, complementing BK5 | Tet$^r$ | This work |
| pMRC | 6.0-kb *Eco*RI fragment in pLAFR1, complementing MR2 and IJ1 | Tet$^r$ | This work |
| pS33 | 10-kb *Bam*HI fragment in pRK404, complementing SS33, SS1, and SS2 | Tet$^r$ | This work |

[a] *R. capsulatus* MT1131 (Rif$^r$ *crtD*) is referred to as "wild type," since it is wild type with respect to its cyt *c* profile and growth properties. MT1131 was originally isolated as a green derivative of *R. capsulatus* SB1003 (40).
[b] Uncharacterized mutations in *ccoNOQP*.

## RESULTS

**Isolation and phenotypic characterization of NADI$^-$ mutants of *R. capsulatus*.** About 30,000 mutagenized colonies of the wild-type *R. capsulatus* strain MT1131 were screened after EMS mutagenesis, and 25 independent mutants unable to perform the NADI reaction at a wild-type level (i.e., turn blue in less than 30 s) but proficient in both Res and Ps growth were retained. Among these mutants, 8 (DM2, MR2, IJ1, IW3, TP1, TP2, SS1, and SS2) exhibited an NADI-slow phenotype (i.e., required an incubation time longer than 2 min to turn blue), while the remaining 17 were completely NADI$^-$ (i.e., no blue color formed within 30 min) (Table 1). These new mutants, together with M7G and M4 previously described (29), were analyzed for their membrane-bound *c*-type cyt profiles, the presence of the subunit I antigen, and their TMPD-induced oxygen consumption activities.

With a Schägger-type SDS-PAGE system (39), four distinct membrane-bound *c*-type cyts, with approximate molecular masses of 32, 31, 29, and 28 kDa, are readily detected in chromatophore membranes of the wild-type *R. capsulatus* strain MT1131 grown semiaerobically in MPYE-enriched medium (Fig. 2). Of these cyts, the 31-kDa protein is the cyt $c_1$ subunit of the cyt $bc_1$ complex (15, 22), and the 29-kDa protein is the membrane-associated electron carrier cyt $c_y$ (21). The two remaining cyts of 32 and 28 kDa (cyts $c_p$ and $c_o$, respectively) correspond to the heme *c*-containing subunits of the cyt $cbb_3$ oxidase (15). In comparison with MT1131, chromatophore membranes of the mutants M7G and M4 showed significant differences in their cyt *c* profile (Fig. 2). In M7G, the 32-kDa subunit CcoP (cyt $c_p$) was missing, while the 28-kDa subunit CcoO (cyt $c_o$) was present at almost wild-type amounts. This feature clearly distinguished it from M4, which lacks both of these cyt *c* subunits of cyt $cbb_3$ oxidase. On the other hand, the cyt *c* profiles of the majority of the newly isolated NADI$^-$ mutants were identical to that of M4 (i.e., the cyt *c* subunits of cyt $cbb_3$ oxidase were undetectable), while only two of them, BK5 and GK1, had all *c*-type cyts present (Fig. 2 and Table 2). In addition, GK1 exhibited a growth medium-dependent NADI$^-$ phenotype, in that it was NADI slow on the minimal medium Med A while NADI$^-$ on the enriched medium MPYE. The NADI-slow mutants SS1, SS2, IW3, TP1, and TP2 contained small amounts of CcoP and CcoO, while MR2 and IJ1 had reduced amounts of all membrane-bound *c*-type cytochromes. The presence of subunit I (CcoN) of the cyt $cbb_3$ oxidase in these mutants was tested with polyclonal antibodies raised against purified CcoN obtained from *R. capsulatus* MT1131, as described in Materials and Methods. Western blot analyses revealed that CcoN was absent in all M4-like mutants (Fig. 2), establishing that they lacked all subunits of the cyt $cbb_3$ oxidase. On the other hand, CcoN was present in M7G, BK5, and GK1 at, or close to, wild-type levels, while the NADI-slow mutants SS1, SS2, IW3, IJ1, and MR2, in agreement with their cyt *c* profiles and NADI phenotypes, had a significantly reduced amount of CcoN (Table 2 and data not shown).

Oxygen consumption rates of chromatophore membranes of the wild type and NADI$^-$ mutants were measured polarographically in the presence of ascorbate and TMPD. With the exception of GK1, MR2, and IJ1, less than 5% of the wild-type activity was detectable in all mutants, confirming their cyt *c* oxidase$^-$ phenotype (Table 3). On the other hand, MR2 and IJ1 showed about 20% of the wild-type cyt $cbb_3$ oxidase and cyt $bc_1$ complex activities, in agreement with their NADI-slow phenotype and the reduced amounts of all membrane-bound cyts. The chromatophore membranes derived from GK1 grown on MPYE medium had less than 5% of the wild-type activity, while those obtained from cells grown on Med A exhibited more than 15% of the wild-type activity, supporting its growth medium dependent conditional NADI phenotype.

In summary, the overall data revealed two different NADI

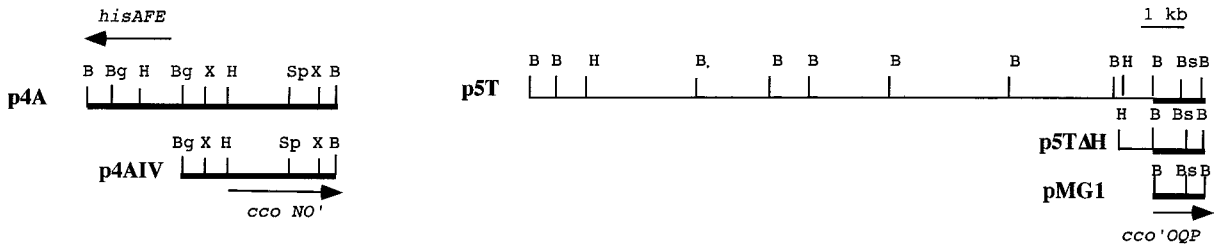


FIG. 1. Physical and genetic map of the plasmids p4A and p5T, complementing the *R. capsulatus* mutants M4 and M7G, respectively. The plasmids p4A1V, derived from p4A, and p5TΔH and pMG1, derived from p5T (see Materials and Methods), are also shown. The locations of *ccoNO* and *ccoOQP* are indicated. B, *Bam*HI; Bg, *Bgl*II; Bs, *Bst*EII; H, *Hin*dIII; X, *Xho*I; Sp, *Sph*I.

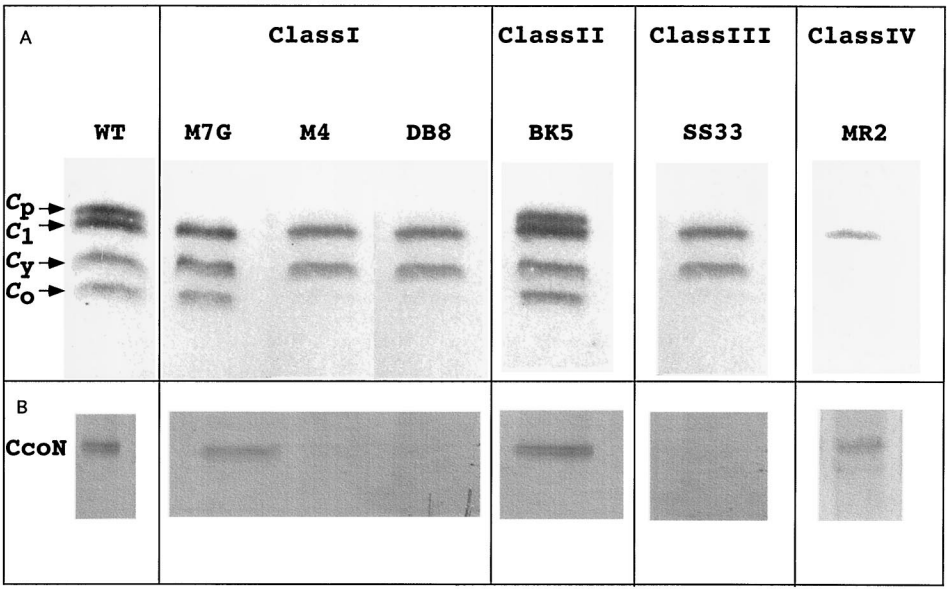


FIG. 2. (A) TMBZ-stained SDS-PAGE analysis of *c*-type cyts from various *R. capsulatus* NADI$^-$ mutants grown on enriched MPYE medium (100 μg of membrane proteins was loaded per lane). (B) Western blot analysis with anti-CcoN (subunit I) antibodies. After SDS-PAGE (10 μg of membrane proteins per lane) and electrophoretic transfer onto an Immobilon-P membrane. CcoN was detected with horseradish peroxidase-conjugated anti-rabbit immunoglobulin G with $NiCl_2$-enhanced 3,3′-diaminobenzidine as the substrate. Cyts $c_p$ and $c_o$ are the subunits II and III of cyt $cbb_3$ oxidase, and cyts $c_1$ and $c_y$ correspond to the cyt $c_1$ subunit of the $bc_1$ complex and the membrane-attached electron carrier $c_y$, respectively.

phenotypes (NADI$^-$ and NADI slow) and three different cyt *c* profiles, in addition to that of M7G (i.e., the presence of CcoN and CcoO in the absence of CcoP), which was exceptional.

**Genetic complementation of NADI$^-$ mutants of *R. capsulatus*.** A transferable *Bam*HI chromosomal library of *R. capsulatus* wild-type strain MT1131 in pRK404 was used to identify the genes required for the activity of cyt $cbb_3$ oxidase. Genetic complementation of M4 and M7G to the NADI$^+$ phenotype yielded two plasmids, p4A and p5T, respectively. The plasmid p5T contained a 16.5-kb chromosomal DNA with multiple internal *Bam*HI sites and was unable to complement M4. Deletion of its various fragments led to p5TΔH (Fig. 1), which contained only a 2.2-kb *Hin*dIII-*Bam*HI fragment sufficient to complement M7G. The plasmid p4A on the other hand, contained a 5.8-kb *Bam*HI fragment without any internal *Bam*HI sites and was also unable to complement M7G. To define the portion of p4A complementing M4, several subclones were constructed (not shown), and of these, p4AIV containing a 3.4-kb *Bgl*II-*Bam*HI fragment (Fig. 1) was able to complement M4 to NADI$^+$. The plasmids p4A and p5TΔH were also tested for their ability to complement all other NADI$^-$ mutants (Table 2). Two of these mutants, DB8 and OH2, were complemented by p5TΔH but not by p4A, and, interestingly, both of them exhibited a cyt $cbb_3$ oxidase subunit profile identical to that of M4 and unlike that of M7G. On the other hand, four mutants, BK4, SS24, SS25, and IW2, were complemented by p4A but not by p5TΔH, while the remaining mutants were not complemented by either of these plasmids (Table 2).

The complete DNA sequences of the 2.2-kb *Hin*dIII-*Bam*HI fragment of p5TΔH and the 5.8-kb *Bam*HI fragment of p4A were determined. Data bank searches indicated that the predicted translation products of two ORFs located in p5TΔH were nearly identical to *ccoQ* and *ccoP* of *R. capsulatus* (45). In addition, the carboxyl terminus (amino acid residues 187 to 242) of *ccoO* of *R. capsulatus* (45) was identified upstream of *ccoQ*, although this homology ended at the internal *Bam*HI site of p5TΔH (Fig. 1). Instead, the carboxyl terminus of another ORF, homologous to ORF2 of the *atp* operon of *Rhodospirillum rubrum* (11) was present in the adjacent *Bam*HI fragment. Considering that the *ccoNOQP* and *atp* operons of *R. capsulatus* are not adjacent to each other (29a), this finding suggested that the two *Bam*HI fragments of p5TΔH were not collinear with their chromosomal counterparts. This was later confirmed by sequencing a PCR product obtained from MT1131 genomic DNA containing the intact *ccoNOQP* cluster (data not shown). In addition, the absence of an internal promoter within the 1.3-kb *Bam*HI fragment in p5TΔH was demonstrated by using pRHK8 and pRHK9 as described in Materials and Methods. Of these plasmids, only pRHK9, which carried this fragment in the same orientation as that in p5TΔH, was able to complement M7G to NADI$^+$. The nucleotide sequence of p4A revealed at least five ORFs with appropriate *R. capsulatus* codon usage. Sequence comparisons revealed that the first three ORFs were homologous to *hisAFE* of *R. sphaeroides* which are involved in histidine biosynthesis (E. Oriol [33], GenBank accession no. X87256) (Fig. 1). The ORF downstream of *hisE* was highly homologous to ORF277 of *R. sphaeroides* and ORF278 of *P. denitrificans* (9, 55) located upstream of most *cco(fix)NOQP* operons. Next to ORF277, *ccoN* and part of *ccoO* (corresponding to amino acid residues 1 to 186) were identified (Fig. 1). These findings indicated that if the two appropriate *Bam*HI fragments of p4A and p5TΔH were adjacent, then they should yield a functional copy of *ccoO*, which was then confirmed by the construction of pOX15 (Fig. 3) as described in Materials and Methods. pOX15 complemented M7G, M4, and all other NADI$^-$ mutants previously complemented by either p4A or p5TΔH, as well as three of the remaining NADI$^-$ mutants (MR1, OH1, and GK2), which were not complemented by either p4A or p5TΔH. In addition, it also yielded about fivefold-higher cyt *c* oxidase activity than a wild-type strain when introduced into MT1131 (Table 3). The overall complementation data therefore demonstrated that M7G, DB8, and OH2 contained a defective copy of *ccoP*; M4,

TABLE 2. Phenotypic and genetic characterization of NADI$^-$ mutants of *R. capsulatus*[a]

| Mutant[b] | Complementation[c] | | | | | | Detection by anti-ccoN antibodies | cyt *c* profile[d] | | | | |
|---|---|---|---|---|---|---|---|---|---|---|---|---|
| | p5TΔH | p4A | pOX15 | pBK1 | pS33 | pMRC | | $c_p$ | $c_1$ | $c_y$ | $c_o$ | $c_2$ |
| Class I | | | | | | | | | | | | |
| M4 | − | + | + | − | − | − | − | − | + | + | − | + |
| BK4 | − | + | + | − | − | − | − | − | + | + | − | + |
| GK2 | − | − | + | − | − | − | NT[e] | − | + | + | − | + |
| MR1 | − | − | + | − | − | − | − | − | + | + | − | + |
| M7G | + | − | + | − | − | − | + | − | + | + | + | + |
| MG1 | + | − | + | − | − | − | − | − | + | + | − | + |
| OH2 | + | − | + | − | − | − | − | − | + | + | − | + |
| DB8 | + | − | + | − | − | − | − | − | + | + | − | + |
| GK32 | − | − | + | − | − | − | − | − | + | + | − | + |
| Class II; BK5 | − | − | − | + | − | − | + | + | + | + | + | + |
| Class III | | | | | | | | | | | | |
| SS33 | − | − | − | − | + | − | − | − | + | + | − | + |
| SS1[f] | − | − | − | − | + | − | (−) | (−) | + | + | (−) | + |
| SS2[f] | − | − | − | − | + | − | (−) | (−) | + | + | (−) | + |
| Class IV | | | | | | | | | | | | |
| MR2[g] | − | − | − | − | − | + | (+) | (+) | (+) | − | (+) | (+) |
| IJ1[g] | − | − | − | − | − | + | (+) | (+) | (+) | − | (+) | (+) |

[a] −, negative; +, positive.
[b] In addition to the mutants listed above, OH1, SS24, SS25, IW2, Sev1, Sev2, Sev3, Sev4, and Sev5 were also classified as class I mutants, since they were complemented by pOX15.
[c] For a detailed description of the complementing plasmids, see the text.
[d] Based on TMBZ-stained SDS-PAGE.
[e] NT, not tested.
[f] Traces of CcoN, CcoP, and CcoO [(−)] were detectable.
[g] Small amounts of CcoN, CcoP, and CcoO [(+)] were detectable.

BK4, SS24, SS25, and IW2 contained a defective copy of *ccoN*; and MR1, OH1, and GK2 contained a defective copy of *ccoO*.

PCR products obtained with the chromosomal DNA of different mutants as a template were sequenced to determine the molecular nature of the different mutations (Fig. 3). These analyses revealed that in the case of M4, the mutation was an in-frame deletion between alanine 117 and alanine 141 of CcoN. In MR1, a mutation substituting tryptophan for arginine 107 of CcoO was found, and in the case of M7G and OH2, the tryptophan 267 and tryptophan 34 of CcoP, respectively, were changed to stop codons (TGA). On the other hand, since DB8 was isolated after Tn*5* mutagenesis, a Kan$^r$-mediating fragment of its chromosomal DNA was first cloned into pBSII, and sequence analysis identified the Tn*5* insertion after glycine 15 of CcoP (Fig. 3). These data pointed out that the CcoP$^-$ mutants like OH2, DB8, and MG1, which lacked all subunits of cyt $cbb_3$ oxidase, contained nonsense mutations early in *ccoP*, preventing them from producing any sizeable fragment of CcoP, while M7G which contained both CcoN and CcoO, had a similar mutation located only 28 amino acid residues away from the carboxyl-terminal end of CcoP. Thus, the CcoP$^-$ mutants exhibited two distinct cyt $cbb_3$ subunit profiles, either containing CcoO (like M7G) or lacking it (like MG1, DB8, and OH2). Finally, the insertion and insertion-deletion mutants MG1 (*ccoP*::*kan*) and GK32 [Δ(*ccoNO*::*kan*)], respectively, obtained as described in Materials and Methods, were also analyzed. Both of these mutants were NADI$^-$ Ps$^+$ and lacked all subunits of cyt $cbb_3$ oxidase like DB8, OH2, MR1, and M4. As expected, while MG1 was complemented by p5TΔH, GK32 could only be complemented by pOX15. All of these mutants were grouped as class I mutants carrying mutations within the structural genes of the cyt $cbb_3$ oxidase of *R. capsulatus*.

A conserved ORF of unknown function, named ORF277 or ORF278 in different species, is located immediately upstream of *cco(fix)NOQP*. To find out whether ORF277 is required for cyt $cbb_3$ oxidase activity, two mutants containing insertion mutations, GK277-1 and GK277-2, were constructed (Fig. 3). Both of these mutants were NADI$^+$ on both minimal medium Med A and enriched medium MPYE, grew like the wild type under both Ps and Res growth conditions, and had cyt $cbb_3$ subunit profiles and oxygen uptake activities similar to those of a wild-type strain (Table 3 and data not shown). Therefore, ORF277 is not required for cyt $cbb_3$ oxidase activity or assembly and is not involved in Ps or Res energy transduction in *R. capsulatus* under the growth conditions tested.

**NADI$^-$ mutants not complemented by *ccoNOQP*.** Of the newly described 25 NADI$^-$ mutants, 11 (BK5, GK1, SS33, SS1, SS2, MR2, IJ1, DM2, IW3, TP1, and TP2) were not complemented by pOX15 carrying *ccoNOQP* (Table 2). A *lacZ*::*ccoN* translational fusion was then used to differentiate among them those that affected the assembly or biogenesis of cyt $cbb_3$ oxidase. All of the mutants tested, including GK1, which had a growth medium-dependent NADI phenotype, exhibited wild-type amounts of the β-galactosidase activity under both Ps and Res growth conditions on both enriched and minimal media. These data indicated that they affected the assembly or biogenesis of the cyt $cbb_3$ oxidase rather than the expression of *ccoNOQP*. Plasmids complementing the mutants BK5 and SS33 to the NADI$^+$ phenotype were sought with the *R. capsulatus* MT1131 *Bam*HI and *Hin*dIII chromosomal libraries, and pBK1 containing a 4.5-kb *Hin*dIII fragment and pS33 containing a 10-kb *Bam*HI fragment were obtained (Table 2). While the latter plasmid also complemented SS1 and SS2, the mutants MR2 and IJ1 were not complemented by either of them. These mutants were also phenotypically distinct from the others, since they not only had small amounts of active cyt

TABLE 3. TMPD oxidase activities in chromatophores from various *R. capsulatus* mutants grown chemoheterotrophically in MPYE medium

| Strain | Sp act (μmol of $O_2$/h/mg of protein)[a] | | % of wild-type activity |
|---|---|---|---|
| | Ascorbate-TMPD | + KCN | |
| MT1131 | 34.47 | 0.98 | 100 |
| MT1131/pOX15 | 183.6 | 0.2 | 532 |
| GK277-1 | 31.4 | 0.7 | 91 |
| GK277-2 | 28.8 | 0.2 | 83.6 |
| Mutants | | | |
| Class I | | | |
| GK32 | 0.5 | 0.5 | 0 |
| M4 | 0.6 | 0.45 | 1.8 |
| BK4 | 0 | 0 | 0 |
| MR1 | 1.6 | 0.38 | 1.1 |
| DB8 | 0.54 | 0.54 | 0 |
| OH2 | 1.2 | 0.83 | 1.1 |
| MG1 | 0.2 | 0.1 | 0.3 |
| M7G | 0.97 | 0.24 | 2.1 |
| Class II, BK5 | 0.9 | 0.65 | 0.73 |
| Class III | | | |
| SS33 | 0.3 | 0.11 | 0.6 |
| SS1 | 1.5 | 0.15 | 3.9 |
| SS2 | 1.6 | 0.25 | 3.9 |
| Class IV | | | |
| MR2 | 6.5 | 0.8 | 16.6 |
| IJ1 | 7.2 | 0.6 | 19.2 |
| Unclassified | | | |
| GK1 (MPYE) | 0.8 | 0.35 | 1.3 |
| GK1 (Med A) | 5.6 | 0.21 | 16 |
| IW3 | 1.7 | 0.25 | 4.0 |

[a] Values shown are means of at least three independent measurements. Note that the activity found in GK1 is dependent on the growth medium.

$cbb_3$ oxidase and cyt $bc_1$ complex, but they also lacked the membrane-bound electron carrier cyt $c_y$ (17, 21) (Table 2 and Fig. 2). A plasmid, pMRC, complementing them exclusively was also isolated and is currently under study. Finally, the remaining five NADI$^-$ mutants, GK1, DM2, TP1, TP2, and IW3, could not be complemented by either pOX15, pBK1, pS33, or pMRC and may define additional genes required for the biogenesis of the cyt $cbb_3$ oxidase of *R. capsulatus.*

In summary, the availability of the different mutants and the plasmids complementing them genetically, in addition to their different cyt *c* profiles, clearly established that in *R. capsulatus*, the presence of an active cyt $cbb_3$ oxidase requires several additional gene products distinct from its structural genes.

## DISCUSSION

*R. capsulatus* is unique in comparison to other phylogenetically related species, like *R. sphaeroides* and *P. denitrificans*, in that it has no $aa_3$-type cyt *c* oxidase (14, 16, 26, 54). Thus, its inability to perform the NADI reaction is directly linked to a defect in its only cyt *c* oxidase, which is of the $cbb_3$ type (15). The structural genes of this enzyme, *ccoNOQP*, have previously been isolated and sequenced from *R. capsulatus* 37b4 (45). Here, not only were these genes also obtained from a different *R. capsulatus* strain (MT1131), but also the molecular natures of various mutations located in *ccoNOQP* were identified, their effects on the assembly of the cyt $cbb_3$ oxidase were defined, and the genetic organization of the regions flanking these genes was determined. In addition, several classes of *R. capsulatus* mutations located outside of *ccoNOQP* and affecting the biogenesis of cyt $cbb_3$ oxidase were isolated.

In a recent study, Zufferey et al. (57) have analyzed the assembly of the cyt $cbb_3$ oxidase in *Bradyrhizobium japonicum* and proposed an ordered biogenesis pathway for it. According to this work, an insertion mutation at the amino terminus of Fix(Cco)P, results in a stable Fix(Cco)NO core complex with residual TMPD-induced oxygen uptake activity in the absence of Fix(Cco)P. Thus, in this species, Fix(Cco)N and Fix(Cco)O may form a catalytically active subcomplex, and Fix(Cco)P is apparently not essential for cyt $cbb_3$ oxidase activity. The situation is different in *R. capsulatus*, since in three CcoP$^-$ mutants of this species (DB8, MG1, and OH2) carrying mutations located at various positions in *ccoP*, none of the individual subunits of cyt $cbb_3$ oxidase, nor any oxygen uptake activity, could be detected. Only in M7G, which contained a mutation located at the very carboxyl-terminal end of CcoP, could a subunit profile similar to that observed in the Fix(Cco)P$^-$ mutant of *B. japonicum* be seen. However, even in this mutant producing the CcoN and CcoO subunits of the cyt $cbb_3$ oxidase, no TMPD-induced oxygen uptake activity could be detected. Furthermore, previous biochemical characterizations have demonstrated that the low-spin heme $b(b_{410})$ group associated with the subunit I of cyt $cbb_3$ oxidase is also undetectable in M7G (15), which is in agreement with the absence of TMPD-induced oxygen uptake. Why M7G contains nonfunctional CcoN and CcoO is unclear. One possibility is that the

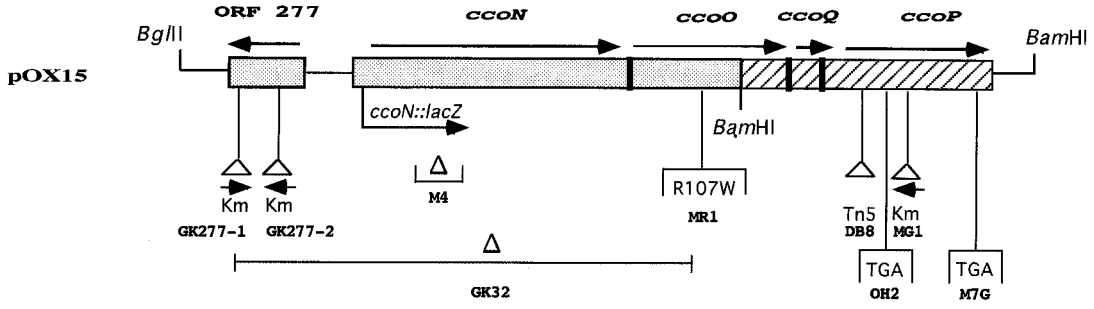


FIG. 3. Physical and genetic map of plasmid pOX15 carrying *ccoNOQP*. pOX15 was constructed by ligation of the 1.3-kb *Bam*HI fragment of pMG1 into the *Bam*HI site of p4AIV as described in Materials and Methods. The orientation of ORF277 and *ccoNOQP* and the location of the mutations in different EMS-induced or constructed NADI$^-$ mutants of *R. capsulatus* are also indicated. Km, Tn*5*, Δ, and TGA correspond to the kanamycin resistance gene, transposon Tn*5*, deletion, and stop codon, respectively; arrowheads refer to the orientation of the insertion mutations.

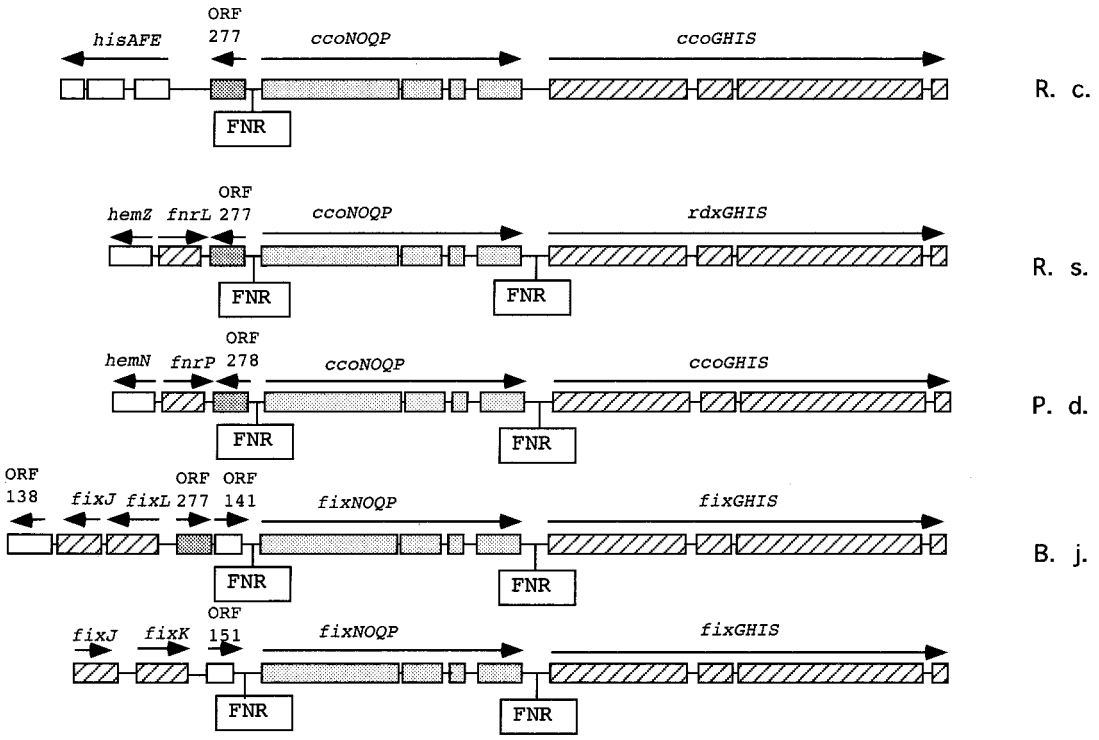


FIG. 4. Comparison of the genetic organization of the *cco(fix)NOQP* operons and their flanking regions in different organisms. FNR indicates the presence of possible Fnr-binding sites in the intergenic regions upstream and downstream of the *cco(fix)NOQP* operons. The *hisAFE* genes are involved in histidine biosynthesis, and *fnrL* and *fnrP* are *fnr*-like genes most likely involved in oxygen- or redox-regulated expression of cyt $cbb_3$ oxidase. *fixJ*, *fixK*, and *fixL* code for oxygen response elements in *B. japonicum*. *hemZ* and *hemN* correspond to the genes encoding the anaerobic coporphyrinogen III oxidase. R.c., *R. capsulatus*; R.s., *R. sphaeroides*; P.d., *P. denitrificans*; B.j., *B. japonicum*. The bottom region (not labeled) represents *R. meliloti.*

carboxyl-terminally truncated form of CcoP synthesized in this mutant may still allow the assembly of cyt $cbb_3$ oxidase, albeit with its subsequent proteolytic degradation, explaining its steady-state absence in the chromatophore membranes. In any event, the phenotypes of the $CcoP^-$ mutants and the steady-state presence of the various subunits of cyt $cbb_3$ oxidase differ between *R. capsulatus* and *B. japonicum*. In addition, our current data in combination with previous work on M7G (15) suggest that the low-spin heme group is also not essential for the stability of *R. capsulatus* cyt $cbb_3$ oxidase, as it has been shown for *R. sphaeroides* cyt $aa_3$ oxidase (19). Again, this is unlike *B. japonicum*, where the cyt $cbb_3$ oxidase becomes unstable if its putative low-spin heme ligand H131 is substituted for by an alanine (58). Taken together, the data presented in this work clearly suggest an important role for CcoP in the assembly and activity of the cyt $cbb_3$ oxidase in *R. capsulatus*, unlike in *B. japonicum*, where this subunit appears to be dispensable.

In the case of the $CcoO^-$ mutant MR1, a conserved arginine is replaced by a tryptophan, leading to the absence of all subunits of the cyt $cbb_3$ oxidase. Considering that CcoO shows no homology to any other known cyts besides the Cco(Fix)O proteins of other organisms, the question of whether this residue is important not only for the enzyme activity but also for the assembly or the steady-state stability of cyt $cbb_3$ oxidase remains to be probed further. In comparison to subunit I of cyt $aa_3$ oxidases, which has 12 transmembrane α-helices organized in a threefold symmetry (20, 47), CcoN (subunit I) of the cyt $cbb_3$ oxidase has 14 putative α-transmembrane helices. However, β-galactosidase and alkaline phosphatase fusion studies with *B. japonicum* indicated that the first two hydrophobic stretches are located in the cytoplasm (58), suggesting that its topology is similar to that of subunit I of cyt $aa_3$ oxidases (14, 16). Of these transmembrane helices, the second one spans residues 113 to 133, is highly conserved in all Cco(Fix)N proteins (9, 24, 34, 55), and contains a conserved histidine (H114) as a putative ligand of the low-spin heme. The *R. capsulatus* $NADI^-$ mutant M4 contains an in-frame deletion covering the amino acid residues 117 to 141 and lacks all subunits of the cyt $cbb_3$ oxidase, suggesting that the second transmembrane helix of subunit I (residues 113 to 133) is required for the assembly and stability of the *R. capsulatus* enzyme. In addition, it is noteworthy that the *ccoNOQP* mutants of *R. capsulatus* MT1131 described in this study do not affect the presence of cyt $c_1$ or $c_y$. This is in contrast to the results obtained with *R. capsulatus* 37b4, in which a *ccoN* mutation significantly reduces the amounts of all membrane-bound cytochromes (45).

The presence of multiple terminal oxidases necessitates a complex regulatory network to initiate the biosynthesis of a particular oxidase in response to different intra- and extracellular signals. Studies with rhizobial species have shown that cyt $cbb_3$ oxidase is required for microaerobic respiration in endosymbiotic bacteroids (34), where its high oxygen affinity allows respiration at low oxygen concentrations (36). In rhizobial species, the oxygen sensors *fixLJ* and *fixK* are located upstream of *fixNOQP* encoding cyt $cbb_3$ oxidase (4, 12, 34), and putative regulatory DNA sequences with dyad symmetry are present upstream of *fixN*. In *P. denitrificans* and *R. sphaeroides*, other oxygen response regulators, the *fnr*-like genes *fnrP* and *fnrL*, respectively, are located upstream of *ccoNOQP* (8, 55). In addition, Fnr binding consensus sequences have been identified in the intergenic region between ORF277 and *ccoN* in

both organisms (8, 48, 55, 56). Putative Fnr binding sequences (TTGAT-N4-GTCAA at positions −91 to −108 and TTGAC-N4-ATCA at positions −168 to −181 from the first ATG codon of *ccoN*) are also present in the ORF277-*ccoN* intergenic region of *R. capsulatus* (Fig. 4). However, in contrast to the other related species, an ORF containing a gene coding for a possible Fnr-like protein is absent upstream of *ccoNOQP* in *R. capsulatus*. Instead, three ORFs with strong homologies to the *hisAFE* of *R. sphaeroides* were identified. Furthermore, a gene probably encoding an anaerobic coporphyrinogen III oxidase (*hemZ* in *R. sphaeroides* and *hemN* in *P. denitrificans*), which is located upstream of the *fnr*-like genes in both of these species (56), is also absent in the upstream region of *ccoNOQP* of *R. capsulatus* (Fig. 4).

In *R. sphaeroides*, *P. denitrificans*, and rhizobial species, a presumably copper-specific transport operon, called *rdxBHIS*, *ccoGHIS*, and *fixGHIS*, respectively, is located downstream of *cco(fix)NOQP* (9, 23, 32, 35). A similar gene cluster is also present in *R. capsulatus* (Fig. 4 and data not shown). In the *cco(fix)P-cco(fix)G* intergenic region, Fnr-like DNA-binding sites are located in *B. japonicum*, *Rhizobium meliloti*, *P. denitrificans*, and *R. sphaeroides*, suggesting that in these species, the expression of both *cco(fix)NOQP* and *cco(fix)GHIS* clusters is coregulated by Fnr. Interestingly, no Fnr binding site is present in the *ccoP-ccoG* intergenic region of *R. capsulatus*. This finding, along with the differences in the upstream region of *ccoNOQP* described above, suggests that a different mode of regulation for both *ccoNOQP* and *ccoGHIS* may be operational in *R. capsulatus*. Considering that in many facultative aerobes an oxygen (or redox)-regulated switch may turn on and off various cyt *c* oxidases with different oxygen affinities (6, 9, 48), it is tempting to speculate that cyt $cbb_3$ oxidase in *R. capsulatus* supports aerobic growth under both high and low oxygen concentrations.

As in *R. sphaeroides* and *P. denitrificans*, an ORF, potentially coding for a polypeptide of 277 amino acids with a signal sequence-like transmembrane helix (37), is located upstream of *R. capsulatus ccoNOQP*. However, its homolog is not present upstream of *fixNOQP* of *R. meliloti* (5), and in *B. japonicum*, ORF277 is separated from *fixNOQP* by an additional ORF (ORF141) (34). Despite its conservation, ORF277 is apparently not essential for either cyt $cbb_3$ oxidase activity or for Res and Ps energy transduction in *R. capsulatus*. Its mutational inactivation has no obvious effect on NADI reaction, oxygen uptake, cyt *c* profile, Res, or Ps growth of this species under the conditions tested, and its function, if any, remains unknown.

In summary, while the majority of the newly isolated NADI mutations of *R. capsulatus* were found to be located in *cco NOQP* encoding the structural genes of cyt $cbb_3$ oxidase, many others located elsewhere and affecting the activity of this enzyme were also isolated. Ongoing biochemical and genetic characterizations of these mutants reveal that at least four additional gene products are required at some posttranslational steps for the presence of an active cyt $cbb_3$ oxidase in *R. capsulatus*. Their future studies will undoubtedly help us to better understand the assembly and steady-state stability of this and other multicomponent membrane-associated, energy-transducing enzyme complexes.

## ACKNOWLEDGMENTS

This work was supported by grants 91ER20052 from DOE and GM38237 from NIH.

We thank G. Brasseur and S. Mandaci for the isolation of many NADI$^-$ mutants and Z.-S. Li for valuable help with protein purification. The contribution of M. Grooms to the isolation of the plasmids p5T and p4A is gratefully acknowledged. We also thank H. Myllykallio for stimulating discussions.

## REFERENCES

1. **Adams, C. W., M. E. Forrest, S. N. Cohen, and J. T. Beatty.** 1989. Structural and functional analysis of transcriptional control of the *Rhodobacter capsulatus puf* operon. J. Bacteriol. **171:**473–482.
2. **Altschul, S. F., W. Gish, W. Miller, E. W. Myers, and D. J. Lipman.** 1990. Basic local alignment search tool. J. Mol. Biol. **215:**403–410.
3. **Baccarini-Melandri, A., D. Zannoni, and B. A. Melandri.** 1973. Energy transduction in photosynthetic bacteria. IV. Respiratory sites and energy conservation in membranes from dark-grown cells of *Rhodopseudomonas capsulata*. Biochim. Biophys. Acta **314:**298–313.
4. **Batut, J., and P. Boistard.** 1994. Oxygen control in *Rhizobium*. Antonie Leeuwenhoek **66:**129–150.
5. **Batut, J., M. Daveran-Mignot, M. David, J. Jacobs, A. M. Garneron, and D. Kahn.** 1989. *fixK*, a gene homologous with *fnr* and *crp* of *Escherichia coli*, regulates nitrogen fixation genes both positively and negatively in *Rhizobium meliloti*. EMBO J. **8:**1279–1286.
6. **Bosma, G., M. Braster, A. H. Stouthamer, and H. W. van Verseveld.** 1987. Subfractionation and characterization of soluble *c*-type cytochromes from *Paracoccus denitrificans* cultured under various limiting conditions in the chemostat. Eur. J. Biochem. **165:**665–670.
7. **Daldal, F., S. Cheng, J. Applebaum, E. Davidson, and R. C. Prince.** 1986. Cytochrome $c_2$ is not essential for photosynthetic growth of *Rhodopseudomonas capsulata*. Proc. Natl. Acad. Sci. USA **83:**2012–2016.
8. **de Gier, J.-W., M. Lübben, W. N. M. Reijnders, C. A. Tipker, D. J. Slotboom, R. J. M. van Spanning, A. H. Stouthammer, and J. van der Oost.** 1994. The terminal oxidases of *Paracoccus denitrificans*. Mol. Microbiol. **13:**183–196.
9. **de Gier, J.-W., M. Schepper, W. N. M. Reijnders, S. J. van Dyck, D. J. Slotboom, A. Warne, M. Saraste, K. Kraab, M. Finel, A. H. Stouthamer, R. J. M. van Spanning, and J. van der Oost.** 1996. Structural and functional analysis of $aa_3$-type and $cbb_3$-type cytochrome *c* oxidase of *Paracoccus denitrificans* reveals significant differences in proton-pump design. Mol. Microbiol. **20:**1247–1260.
10. **Ditta, G., T. Schmidhauser, E. Yacobson, P. Lu, X.-W. Liang, D. R. Finlay, D. Guiney, and D. R. Helsinki.** 1985. Plasmids related to the broad host range vector, pRK290, useful for gene cloning and for monitoring gene expression. Plasmid **13:**149–153.
11. **Falk, G., A. Hampe, and J. E. Walker.** 1985. Nucleotide sequence of the *Rhodospirillum rubrum atp* operon. Biochem. J. **228:**391–407.
12. **Fischer, H.-M.** 1994. Genetic regulation of nitrogen fixation in *Rhizobia*. Microbiol. Rev. **58:**352–386.
13. **Garcia-Horsman, A., E. Berry, J. P. Shapleigh, J. O. Alben, and R. B. Gennis.** 1994. A novel cytochrome *c* oxidase from *Rhodobacter sphaeroides* that lacks $Cu_A$. Biochemistry **33:**3113–3119.
14. **Garcia-Horsman, J. A., B. Barquera, J. Rumbley, J. Ma, and R. B. Gennis.** 1994. The superfamily of heme-copper respiratory oxidases. J. Bacteriol. **176:**5587–5600.
15. **Gray, K. A., M. Grooms, H. Myllykallio, C. Moomaw, C. Slaughter, and F. Daldal.** 1994. *Rhodobacter capsulatus* contains a novel *cb*-type cytochrome *c* oxidase without a $Cu_A$ center. Biochemistry **33:**3120–3127.
16. **Haltia, T., and M. Wikström.** 1992. Cytochrome oxidase: notes on structure and mechanism, p. 217–239. *In* L. Ernster (ed.), Molecular mechanisms in bioenergetics. Elsevier Science Publishers, Amsterdam, The Netherlands.
17. **Hochkoeppler, A., F. E. Jenney, Jr., S. E. Lang, D. Zannoni, and F. Daldal.** 1995. Membrane-associated cytochrome $c_y$ of *Rhodobacter capsulatus* is an electron carrier from the cytochrome $bc_1$ complex to the cytochrome *c* oxidase during respiration. J. Bacteriol. **177:**608–613.
18. **Hoffmann, K., and W. Stoffel.** 1993. TMbase—a database of membrane spanning protein segments. Biol. Chem. Hoppe-Seyler **347:**166.
19. **Hosler, J. P., S. Ferguson-Miller, M. W. Calhoun, J. W. Thomas, J. Hill, L. J. Lemieux, J. Ma, C. Georgiou, J. Fetter, J. Shapleigh, M. M. J. Tecklenburg, G. T. Babcock, and R. B. Gennis.** 1993. Insight into the active-site structure and function of cytochrome oxidase by analysis of site-directed mutants of bacterial cytochrome $aa_3$ oxidase and cytochrome *bo*. J. Bioenerg. Biomembr. **25:**121–136.
20. **Iwata, S., C. Ostermeier, B. Ludwig, and H. Michel.** 1995. Structure at 2.8 Å resolution of cytochrome c oxidase from *Paracoccus denitrificans*. Nature **376:**660–669.
21. **Jenney, F. E., and F. Daldal.** 1993. A novel membrane associated *c*-type cytochrome, cyt $c_y$, can mediate the photosynthetic growth of *Rhodobacter capsulatus* and *Rhodobacter sphaeroides*. EMBO J. **12:**1283–1292.
22. **Jenney, F. E., R. C. Prince, and F. Daldal.** 1994. Roles of the soluble cytochrome $c_2$ and membrane-associated cytochrome $c_y$ of *Rhodobacter capsulatus* in photosynthetic electron transfer. Biochemistry **33:**2496–2502.
23. **Kahn, D., M. David, O. Domergue, M.-L. Daveran, J. Ghai, P. R. Hirsch, and J. Batut.** 1989. *Rhizobium meliloti fixGHI* sequence predicts involvement of a specific cation pump in symbiotic nitrogen fixation. J. Bacteriol. **171:**929–939.
24. **Kahn, D., J. Batut, M.-L. Daveran, and J. Fourment.** 1993. Structure and regulation of the *fixNOQP* operon from *Rhizobium meliloti*, p. 474. *In* R.

Palacios, J. Mora, and W. E. Newton (ed.), New horizons in nitrogen fixation. Kluwer Academic Publishers, Dordrecht, The Netherlands.
25. **Keilin, D.** 1966. The history of cell respiration and cytochrome. Cambridge University Press, Cambridge, United Kingdom.
26. **Klemme, J.-H., and H. G. Schlegel.** 1969. Untersuchungen zum Cytochrom-Oxidase System aus anaerob im Licht und Dunkeln gewachsenen Zellen von *Rhodopseudomonas capsulata*. Arch. Mikrobiol. **68:**326–354.
27. **La Monica, R. F., and B. L. Marrs.** 1976. The branched respiratory system of photosynthetically grown *Rhodopseudomonas capsulata*. Biochim. Biophys. Acta **423:**431–439.
28. **Lowry, O. H., N. J. Rosebrough, A. L. Farr, and R. J. Randall.** 1951. Protein measurement with the Folin phenol reagent. J. Biol. Chem. **193:**265–275.
29. **Marrs, B., and H. Gest.** 1973. Genetic mutations affecting the respiratory electron-transport system of the photosynthetic bacterium *Rhodopseudomonas capsulata*. J. Bacteriol. **114:**1045–1051.
29a. **Melandri, A.** Personal communication.
30. **Meyer, T. E., and T. J. Donohue.** 1995. Cytochromes, iron-sulfur, and copper proteins mediating electron transfer from the cyt $bc_1$ complex to photosynthetic reaction center complexes, p. 725. *In* R. E. Blankenship, M. T. Madigan, and C. E. Bauer (ed.), Anoxygenic photosynthetic bacteria. Kluwer Academic Publishers, Dordrecht, The Netherlands.
31. **Miller, J. H.** 1972. Experiments in molecular genetics. Cold Spring Harbor Laboratory Press, Cold Spring Harbor, N.Y.
32. **O'Gara, J. P., and S. Kaplan.** 1997. Evidence for the role of redox carriers in photosynthesis gene expression and carotenoid biosynthesis in *Rhodobacter sphaeroides* 2.4.1. J. Bacteriol. **179:**1951–1961.
33. **Oriol, E., S. Mendez-Alvarez, J. Barbi, and I. Gibert.** 1996. Cloning of the *Rhodobacter sphaeroides hisI* gene: unifunctionality of the encoded protein and lack of linkage to other *his* genes. Microbiology **142:**2071–2078.
34. **Preisig, O., D. Anthamatten, and H. Hennecke.** 1993. Genes for a microaerobically induced oxidase complex in *Bradyrhizobium japonicum* are essential for a nitrogen-fixing endosymbiosis. Proc. Natl. Acad. Sci. USA **90:**3309–3313.
35. **Preisig, O., R. Zufferey, and H. Hennecke.** 1996. The *Bradyrhizobium japonicum fixGHIS* genes are required for the formation of the high-affinity $cbb_3$-type cytochrome oxidase. Arch. Microbiol. **165:**297–305.
36. **Preisig, O., R. Zufferey, L. Thöny-Meyer, C. A. Appleby, and H. Hennecke.** 1996. A high-affinity $cbb_3$-type cytochrome oxidase terminates the symbiosis-specific respiratory chain of *Bradyrhizobium japonicum*. J. Bacteriol. **178:** 1532–1538.
37. **Pugsley, A. P.** 1993. The complete general secretory pathway in gram-negative bacteria. Microbiol. Rev. **57:**50–108.
38. **Sambrook, J., E. F. Fritsch, and T. Maniatis.** 1989. Molecular cloning: a laboratory manual, 2nd ed. Cold Spring Harbor Laboratory Press, Cold Spring Harbor, N.Y.
39. **Schägger, H., and G. von Jagow.** 1987. Tricine-sodium dodecyl sulfate polyacrylamide gel electrophoresis for the separation of proteins in the range from 1 to 100 kDa. Anal. Biochem. **166:**368–379.
40. **Scolnik, P., M. Walker, and B. L. Marrs.** 1980. Biosynthesis of carotenoids derived from neurosporene in *Rhodopseudomonas capsulata*. J. Biol. Chem. **255:**2427–2432.
41. **Simon, R., U. Priefer, and A. Pühler.** 1983. A broad host range mobilization system for in vivo genetic engineering: transposon mutagenesis in gram-negative bacteria. Bio/Technology **1:**37–45.
42. **Sistrom, W.** 1960. A requirement for sodium in the growth of *Rhodopseudomonas sphaeroides*. J. Gen. Microbiol. **22:**778–785.
43. **Thomas, P. E., D. Ryan, and W. Levin.** 1976. An improved staining procedure for the detection of the peroxidase activity of cytochrome P-450 on sodium dodecyl sulfate polyacrylamide gels. Anal. Biochem. **75:**168–176.
44. **Thompson, J., D. Higgins, and T. Gibson.** 1994. CLUSTAL W: improving the sensitivity of progressive multiple sequence alignment through sequence weighting, position-specific gap penalties and weight matrix choice. Nucleic Acids Res. **22:**4673–4680.
45. **Thöny-Meyer, L., C. Beck, O. Preisig, and H. Hennecke.** 1994. The *ccoNOQP* gene cluster codes for a *cb*-type cytochrome oxidase that functions in aerobic respiration of *Rhodobacter capsulatus*. Mol. Microbiol. **174:**705–716.
46. **Thöny-Meyer, L.** 1997. Biogenesis of respiratory cytochromes in bacteria. Microbiol. Mol. Biol. Rev. **61:**337–376.
47. **Tsukihara, T., H. Aoyama, E. Yamashita, T. Tomizaki, H. Yamaguchi, K. Shizawa-Itoh, R. Nakashima, R. Yaono, and S. Yoshikawa.** 1995. Structures of metal sites of oxidized bovine heart cytochrome *c* oxidase at 2.8 Å. Science **269:**1069–1074.
48. **van Spanning, R. J. M., A. P. N. de Boer, W. N. M. Reijnders, H. V. Westerhoff, A. H. Stouthammer, and J. van der Oost.** 1997. FnrP and NNR of *Paracoccus denitrificans* are both members of the FNR family of transcriptional activators but have distinct roles in respiratory adaptation in response to oxygen limitation. Mol. Microbiol. **23:**893–907.
49. **Wang, J., K. A. Gray, F. Daldal, and D. L. Rousseau.** 1995. The $cbb_3$-type cytochrome *c* oxidase from *Rhodobacter capsulatus* contains a unique active site. J. Am. Chem. Soc. **117:**9363–9364.
50. **Yen, H. C., and B. L. Marrs.** 1977. Growth of *Rhodopseudomonas capsulata* under anaerobic dark conditions with dimethyl sulphoxide. Arch. Biochem. Biophys. **181:**411–418.
51. **Yen, H. C., N. T. Hu, and B. L. Marrs.** 1979. Characterization of the gene transfer agent made by an overproducer mutant of *Rhodopseudomonas capsulata*. J. Mol. Biol. **131:**157–168.
52. **Zannoni, D.** 1995. Aerobic and anaerobic electron transport chains in anoxygenic phototrophic bacteria, p. 949. *In* R. E. Blankenship, M. T. Madigan, and C. E. Bauer (ed.), Anoxygenic photosynthetic bacteria. Kluwer Academic Publishers, Dordrecht, The Netherlands.
53. **Zannoni, D., B. A. Melandri, and A. Baccarini-Melandri.** 1976. Composition and function of the branched oxidase system in wild-type and respiratory mutants of *Rhodopseudomonas capsulata*. Biochim. Biophys. Acta **423:**413–430.
54. **Zannoni, D., A. Baccarini-Melandri, B. A. Melandri, E. H. Evans, R. C. Prince, and A. R. Crofts.** 1974. The nature of the cytochrome *c* oxidase in the respiratory chain of *Rhodopseudomonas capsulata*. FEBS Lett. **48:**152–155.
55. **Zeilstra-Ryalls, J. H., and S. Kaplan.** 1995. Aerobic and anaerobic regulation in *Rhodobacter sphaeroides* 2.4.1: the role of the *fnrL* gene. J. Bacteriol. **177:**6422–6431.
56. **Zeilstra-Ryalls, J. H., and S. Kaplan.** 1996. Control of *hemA* expression in *Rhodobacter sphaeroides* 2.4.1: regulation through alterations in the cellular redox state. J. Bacteriol. **178:**985–993.
57. **Zufferey, R., O. Preisig, H. Hennecke, and L. Thöny-Meyer.** 1996. Assembly and function of the cytochrome $cbb_3$ oxidase subunits in *Bradyrhizobium japonicum*. J. Biol. Chem. **271:**9114–9119.
58. **Zufferey, R., L. Thöny-Meyer, and H. Hennecke.** 1996. Histidine 131, not histidine 43, of the *Bradyrhizobium japonicum* FixN protein is exposed towards the periplasm and essential for the function of the $cbb_3$-type cytochrome oxidase. FEBS Lett. **394:**349–352.